

# A Study of Computational Nontechnology with Nanotubes

**Upendra Sharan Gupta<sup>1</sup>, Aadarsh S Chandran<sup>2</sup>,**

**Abhishek Pahwa<sup>3</sup>, Ayush Awasthi<sup>4</sup>**

*<sup>1</sup>Reader, <sup>2,3,4</sup>UG Scholar, Dept. of Mech .Engineering ,SVITS, Indore (India)*

## **ABSTRACT**

*A narrow window on a very broad field of applications and areas that are opening up and directly fueled by the efforts and advances in the computational nanotechnology based investigations of CNTs. Our paper is focused on the nanomechanics and various properties of nanotubes like thermal properties of CNTs and CNTs in polymer composite materials; chemical reactivity or functionalization of pristine or deformed nanotubes; gas physisorption, diffusion, and storage devices through CNTs; polymer translocation and diffusion in CNT nanochannels for sequencing or drug delivery applications, molecular electronic device components through nanotube heterojunctions, and nanosensors for minuscule amounts of gas and biochemical detection applications, etc. The design of the gears is based on the analogous chemical reactions that are known to occur in bulk phase chemistry. Computational modeling and simulation is useful to investigate the optimal structural, material, and operating conditions*

**Keywords:** Computational Nanotechnologies, Mesoscopic Scale Simulations, Carbon Nanotube

## **I. INTRODUCTION**

The science and technology of nanoscale materials, devices, and their applications in functionally graded materials, molecular electronics, nano computers, sensors, actuators, and molecular machines form the realm of nanotechnology. The prefix “nano” corresponds to a basic unit on a length scale, meaning  $10^{-9}$  meters, which is a hundred to a thousand times smaller than a typical biological cell or bacterium. At few nanometer length scale the devices and systems sizes begin to reach the limit of 10 to 100s of atoms, where even new physical and chemical effects are observed and form the basis for the next generation of cutting edge products based on the ultimate miniaturization where extended atomic or molecular structures form the basic building blocks.

The real progress in nanotechnology, however, has also been spurred by the discovery of atomically precise nanoscale materials such as fullerenes in the mid-1980s and carbon nanotubes in the early 1990s. CNTs, as described in, can be thought of as sheets of carbon rolled up atoms into a tubular structure such that atoms at the seams are connected in a flawless manner according to rules of graphitic ( $sp^2$ ) type chemical bonding. A single sheet of carbon atoms rolled up into a tubular structure is called a Single Wall Carbon Nanotube (SWNT), and a rolled up stack of sheets results in Multiwall Carbon Nanotubes (MWNTs). Since the discovery of MWNTs in 1991 by Iijima [1], and subsequent synthesis of SWNTs by Iijima [2] and Bethune [3], there are numerous experimental and theoretical studies of their electronic, chemical, and mechanical properties [4,5]. CNTs with very good mechanical strength/stiffness and elasticity characteristics, electronic properties ranging from semiconductors to metals, high electronic sensitivity to chemical adsorbates and mechanical strains, and very

large aspect and surface-to-volume ratios have been proposed for applications as reinforcing fibers in functionally graded lightweight composite materials, components of molecular electronic devices, chemical and mechanical sensors and actuators, metrology probe tips, and gas and energy storage materials, respectively [6]. Investigation of the experimental and theory simulation based characterization and conceptualization of novel applications in the above areas are pursued vigorously. The theory and computational modeling of the characterization and application design of CNTs thus has played a significant role in leading the developments from the very beginning.

At nanometer ( $10^{-9}$  m) length scale it is possible to describe the structural, mechanical, thermal, and electronic behavior fairly accurately through computational nanotechnology, i.e., physics and chemistry based modeling and simulations of nanomaterials, devices, and applications. This is perhaps because the devices and systems sizes have shrunk sufficiently on the one hand, and computing power has continued to increase on the other. In many cases, the quantum mechanics based simulation technologies have become also predictive in nature, and many novel concepts and designs were first proposed through modeling and simulations and were then followed by their realization or verification in experiments [7]. Computational nanotechnology is emerging as a fundamental engineering analysis tool for novel nano materials, devices, and systems design in a similar way that the continuum Finite Element Analysis (FEA) was and has been used for design and analysis of micro to macro scale engineering systems such as Integrated Circuits (ICs) and Micro Electromechanical Systems (MEMS) devices in the submillimeter length scale regime and automobiles, airplanes, ships, etc., in large-scale engineering structures.

The computational nanotechnology-based modeling and simulations of CNT nanomechanics, functionally graded composite materials, electronic devices, sensors and actuators, and molecular machines essentially cover the entire range in the multi length and time-scale simulation techniques [7]. For example, simulations of electronic characteristics and sensor applications are very well within the high-accuracy quantum regime, whereas simulations for the processing and characterization of CNT reinforced functional composite materials would typically require mesoscale simulation techniques, which are not yet very well developed. In between there are atomistic simulations for nanomechanics, reactivity, and molecular machines of individual CNTs and Tight Binding (TB) quantum mechanical approaches for the same but at more accurate level. Many of the applications come about through response behavior of the nanoscale materials system to external electromagnetic or thermal fields where the equilibrium response or transport characteristics are simulated for advance prototyping of applications.

## **II. MULTISCALE SIMULATION TECHNIQUES FOR COMPUTATIONAL NANOTECHNOLOGY**

The importance of computational nanotechnology based simulations in advancing the frontiers for the next generation of nanostructured materials, devices, and applications is based on three reasons. First, the length and time scales of important nanoscale systems and phenomenon have shrunk to the level where they can be directly addressed with high fidelity computer simulations and theoretical modeling. Second, the accuracy in the atomistic and quantum mechanical methods has increased to the extent that, in many cases, simulations have

become predictive. Third, the raw CPU power available for routine simulation and analysis continues to increase so that it is regularly feasible to introduce more and more “reality” in the simulation-based characterization and application design. The relevant problems for modeling and simulation based investigations of CNTs are truly multiple length and time scale in nature. At the atomistic level, there are accurate semi classical and quantum simulation methods that feed into the large scale classical Molecular Dynamics (MD) simulations with 10s of millions of atoms, which then can be coupled to mesoscopic (few hundreds of a nanometer length scale) devices and systems. There have been many attempts to develop an integrated “grand simulation tool” based approach that cuts across different length scales on one hand and attempts to achieve a seamless integration across the interfaces on the other [8,9]. In reality, most of these integration schemes are geared toward and work only for very specific materials and devices but do not work otherwise. In the past few years, attempts, however, have also been made on attacking the “right” type of problems with appropriate “right” type of techniques [7] across a wide range of CNT characterization and application simulations. In this section, we briefly summarize the main simulation approaches that have been used in investigating CNTs across many different length and time scales.

## **2.1 Quantum Electronic Structure and Dynamics**

Starting from the bottom up, a few tens to hundreds of atoms are very accurately simulated with the ab initio (or first principles) quantum mechanics based methods, wherein simulations are aimed toward the solution of the complex quantum many body Schrodinger equation of the atomic system (including nuclei and electrons), using numerical algorithms [10]. The atoms are described as a collection of quantum mechanical particles, nuclei and electrons, governed by the Schrodinger equation,  $H \Phi[\{R_i, r\}] = E_{\text{tot}} \Phi[\{R_i, r\}]$ , with the full quantum many body Hamiltonian operator  $H = P^2/2M_i + Z_i e^2/R_i + p^2/2me + e^2/r - Z_i e^2/|R_i - r|$ , where  $R_i$  and  $r$  are nuclei and electron coordinates. Using the Born-Oppenheimer approximation, the electronic degrees of freedom are assumed to follow adiabatically the corresponding nuclear positions, and the nuclei coordinates become classical variables. With this approximation, the full quantum many-body problem is reduced to a quantum many electron problem  $H[R_i] \Psi[r] = E_e \Psi[r]$ , where  $H = \sum_i P_i^2/2M_i + H[R_i]$ ,  $H[R_i]$  is electronic Hamiltonian Operator.

Current ab initio simulation methods are based on a rigorous mathematical foundation of the density functional theory (DFT) [11,12]. This is derived from the fact that the ground state total electronic energy is a functional of the density of the system. Kohn and Sham [11,12] have shown that the DFT can be reformulated as single-electron problem with self-consistent effective potential including all the exchange correlation effects of electronic interactions:

$$H_1 = p^2/2m_e + V_h(r) + V_{xc}[\rho(r)] + V_{ion-el}(r),$$
$$H_i \Psi(r) = \epsilon \Psi(r), \text{ for all atoms}$$
$$\rho(r) = \sum |\Psi(r)|^2.$$

This single-electron Schrodinger equation is known as Kohn-Sham equation, and the Local Density Approximation (LDA) has been introduced to approximate the unknown effective exchange correlation potential. This DFT-LDA method has been very successful in predicting materials properties without using any

experimental inputs other than the identity of the constituent atoms. The DFT based ab initio methods have proven successful in a variety of simulations involving structural, chemical, and electronic characterization of nanostructured materials such as clusters, fullerenes, nanotubes, and nanowires. For practical applications, the DFT-LDA method is implemented with a pseudopotential approximation and a Plane Wave (PW) basis expansion of single electron wave functions [10] These approximations reduce the electronic structure problem to a self-consistent matrix diagonalization problem. At the end of the iterative matrix diagonalization procedure, the resulting eigen values correspond to the quantum mechanically possible electronic energy states of the system, and the eigen functions contain information about the electronic density distribution in the computed space. One of the popular DFT simulation programs is the Vienna Ab initio Simulation package (VASP), which is available through a license agreement [13].CNTs. For dynamic problems, nonorthogonal tight binding molecular dynamics schemes are more accurate but are not easily converted to order N type and can typically handle only systems with up to a few thousand atoms [16].

In the tight binding model [15], an approximation is made to further simplify the quantum many electron problems. It is assumed that the crystal potential is strong, which is the same as assuming that the ionic potentials are strong so that when an electron is captured by an ion during its motion through the lattice, the electron remains at that site for a long time before leaking, or tunneling, to the next ion site. During the capture interval, the electron orbits primarily around a single ion uninfluenced by other atoms so that its state function is essentially that of an atomic orbital. Most of the time the electron is tightly bound to its own atom. In other words, the atomic orbital is modified only slightly by the other atoms in the solid. The tight binding wave function is, therefore, constructed by taking a linear combination of localized atomic orbitals, modulated by a Bloch wave function phase factor for a periodic lattice. This ensures that an electron in a tight binding level will be found, with equal probability, in any cell of the crystal, because its wave function changes only by the phase factor as it moves from one cell to another. The computational efficiency of the tight binding method derives from the fact that the electronic Hamiltonian  $H[RI]$  can be parameterized. Furthermore, the electronic structure information can be easily extracted from the tight binding Hamiltonian, which in addition also contains the effects of angular forces in a natural way.

## **2.2. Atomistic Structure and Molecular Dynamics Simulations**

For larger size CNT systems (hundreds of thousands of atoms), the classical atomistic or MD simulations, which refer most commonly to the situation wherein the motion of atoms or molecules is treated in approximate finite differential equations of Newtonian mechanics, are used. Except when dealing with very light atoms and very low temperatures, the use of classical MD methods is well justified. In MD simulations the dynamic evolution of the system is governed by Newton's classical equation of motion,  $d^2\mathbf{R}/dt^2 = \mathbf{F} = -dV/d\mathbf{R}$ , which is derived from the classical Hamiltonian of the system,  $H = \sum_i P_i^2/2M_i + V(\{\mathbf{R}\})$ . The atomic forces are derived as analytic derivatives of the interaction energy functions,  $\mathbf{F}(\{\mathbf{R}\}) = -dV/d\mathbf{R}$ , and are used to construct Newton's classical equations of motion, which are second order ordinary differential equations. In its global structure a general MD code typically implements an algorithm to find a numerical solution of a set of coupled first order ordinary differential equations given by the Hamiltonian formulation of Newton's second law [18]. The

equations of motion are numerically integrated forward in finite time steps using a predictor corrector method. The interatomic forces are described with explicit or implicit many body force field functions, using the Embedded Atom Method (EAM) or Modified Embedded Atom Method (MEAM) type functions for metals and semiconductors and Stillinger-Weber (S-W) and/or Tersoff Brenner (T-B) type potentials for semiconductors [19]. The T-B type potentials [20,21] are parameterized for and specially suited for carbon-based systems, such as CNTs, and have been used in a wide variety of scenarios with results in good agreement with experimental observations. One needs to be careful, however, when true chemical changes (involving electronic rearrangements) with large atomic displacements are expected to occur during the dynamics.

### **2.3. Electronic and Thermal Transport Simulations**

The low bias electronic transport can be calculated as a generalization of the Transmission Amplitude  $T(E)$  of an incident electron with energy  $E$  in simple one-dimensional potential barrier problem. The Landauer expression is generally used to obtain quantum conductance from the transmission function  $T(E)$  as a function of the injected electron energy. The transmission function is obtained using the Green's function formalism that has been described in detail recently [23]. In the nanotube devices under current consideration, a connection to the outside world is made through metallic leads. A realistic treatment of a nanotube interaction with metal electrodes must involve a judicious construction of the Green's function and is an involved process. To maintain a consistency in the simulations, it is proper to use the Tight Binding (TB) formulation for both the Hamiltonian and the Green's function. The non orthogonal TB Hamiltonian mentioned above consists of  $N$  by  $N$  matrices, where  $N = N(\text{at}) \times N(\text{orb})$ ,  $N(\text{at})$  is the number of atoms in the embedding subspace, and  $N(\text{orb})$  is the number of orbitals on each atom. Contrary to earlier theoretical works on quantum transport, which use  $N(\text{orb}) = 1$  (only one pi-electron orbital per atom) [24], for accuracy recent calculations have used  $N(\text{orb}) = 9$  that includes 1s, 3p, and 5d orbitals for C and Ni (a representative material for metal leads) interface and  $N(\text{orb}) = 4$  for C atoms [25,26]. For consistency, it is better to use the same TB Hamiltonian to perform full symmetry unconstrained molecular dynamics relaxations for the SWNT systems, which is used for conductivity calculations, because dynamic relaxation is found to have given results significantly different from the cases where dynamic relaxation was not allowed. An efficient transfer matrix formalism for obtaining the quantum conductivity of SWNTs, which makes explicit use of the non orthogonality of the basic functions within the above mentioned nonorthogonal TB scheme [27]. This new formalism allows the symmetry unconstrained structural relaxation and even dynamics in a consistent manner with the same Hamiltonian as used in the quantum conductivity calculations. Additionally, for both the structural relaxation and the quantum conductivity simulations the periodic boundary condition or infinite size approximations are not needed. The method is therefore especially suitable for finite sized CNT systems with doping, defects, and chemical functionalization because the Hamiltonian has been parametrized for a variety of interacting atomic species. Current vs. voltage characteristics of single wall CNTs have been obtained in the presence of topological defects as well as chemical adsorbates [27].

The thermal transport simulations in CNTs are in the early stages of development. Most of the attempts, so far, have been through direct methods for thermal conductivity simulations. The underlying approach to the

simulation of thermal transport is through MD simulations with the assumption that at room temperature the electronic contribution to the overall thermal conductivity is small and the thermal transport occurs mainly through phonon driven mechanisms. In direct simulation methods [28,29], appropriate heat baths [30] are simulated at the two ends of CNTs resulting in a flux of thermal energy from the hot region of the tube to the cold. The ratio of heat flux and the temperature gradient in equilibrium condition is sufficient to compute the thermal conductivity at the simulation temperature. The analysis of the phonon driven heat flux is also aided by the computations of the phonon spectrum and vibrational amplitudes, which are succinctly described recently for a variety of SWNTs using the MD approach [31]. In bulk semiconductors and nanowires, the response function-based approach has been applied with some success, and a comparison between bulk thermal conductivity computed with direct and response function based approaches has been discussed [32]. The response function based methods so far have not been applied to CNTs, because these forms quasi one dimensional structures and applying direct simulation methods is not too difficult.

### **III. STRUCTURE AND SYMMETRY**

The structure and symmetry of CNTs has been described in detail in. In this section a summary of salient features is provided, which will be used later for understanding some of the characterization and application scenarios that form the focus of this chapter. A SWNT is best described as a rolled up tubular shell of graphene sheet [4–7]. The body of the tubular shell is mainly made of hexagonal rings (in a sheet) of carbon atoms, whereas the ends are capped by dome shaped half fullerene molecules. The natural curvature in the sidewalls is due to the rolling of the sheet into the tubular structure, whereas the curvature in the end caps is due to the presence of topological (pentagonal ring) defects in the otherwise hexagonal structure of the underlying lattice. The role of the pentagonal ring defect is to give a positive (convex) curvature to the surface, which helps in closing of the tube at the two ends and also make the end caps chemically more reactive compared with the cylindrical walls of the CNTs. Later, however, we show that the topological defect free curved structure of the cylindrical walls also has chemical reactivity, that is a function of the natural curvature or strain induced curvature of CNTs. A MWNT, similarly, is a rolled up stack of graphene sheets into concentric SWNTs, with the ends again either capped by half fullerenes or kept open.

A nomenclature (n,m) used to identify each SWNT, in the literature, refers to integer indices of two graphene unit lattice vectors corresponding to the chiral vector of a nanotube [4–7]. Chiral vectors determine the directions along which the graphene sheets are rolled to form tubular shell structures and perpendicular to the tube axis vectors as explained in Reference 4. The nanotubes of type (n,n), are commonly called armchair nanotubes because of the shape perpendicular to the tube axis and have a symmetry along the axis with a short unit cell (0.25 nm) that can be repeated to make the entire section of a long nanotube. Other nanotubes of type (n, 0) are known as zigzag nanotubes because of the shape perpendicular to the axis and also have a short unit cell (0.43 nm) along the axis. All the remaining nanotubes are known as chiral or helical nanotubes that have longer unit cell sizes along the tube axis.

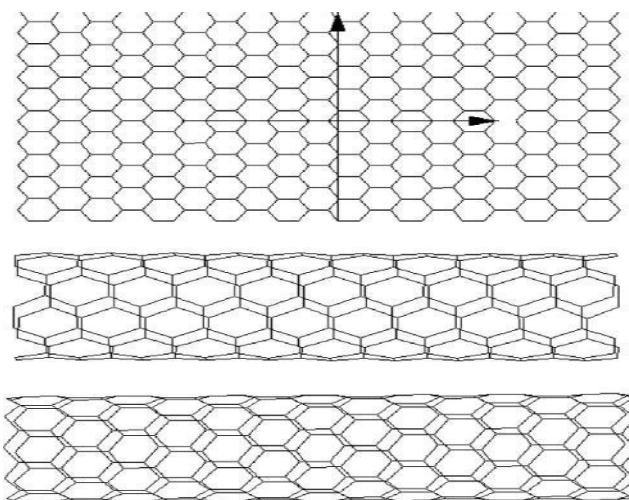


**FIGURE 1 Making of armchair and zigzag carbon nanotubes with (a) rolling directions of a (5,5) armchair nanotube (b) shown with AA and of a (10, 0) zigzag nanotube (c) shown with ZZ**

#### **IV. NANOMECHANICS AND THERMAL PROPERTIES**

The earliest atomistic simulations of CNT mechanics predicted unusually large Young's modulus (of up to 5 Terra Pascal [TPa] or five times larger than the modulus of diamond) and elastic limits (of up to 20 to 30% strain before failure) [33]. These predictions immediately raised the intriguing possibility of applying the nanotubes as super strong reinforcing fibers with few orders of magnitude higher strength and stiffness than any other known material. Subsequently, more accurate simulations using TB molecular dynamics methods and ab initio density functional total energy calculations with realistic strain rate, temperature dependence, and CNT sizes have provided more realistic values of 1 TPa as the Young's modulus and 5 to 10% elastic limit of the tensile strain before failure [34]. In this section, computational modeling and simulation based investigations of the strength and stiffness modulus, plasticity and yielding behavior, vibrational and thermal transport behavior, reinforcing of polymer composites by CNTs and mesoscopic simulations of CNTs are described.

##### **4.1. Modulus of Carbon Nanotubes**

The modulus of the CNTs is a measure of the strength and stiffness against small axial stretching and compression strains as well as nonaxial bending and torsion strains. Contributions to the good elastic mechanical characteristics of CNTs come mainly from the strength of in-plane covalent C-C bonds in graphene sheet and facile out of plane deformations of the structure. For large diameter or small curvature CNTs, the modulus, strength, and stiffness should therefore be comparable with the in plane modulus and strength of graphene sheet. In a tubular geometry, however, the elastic strain energies are also affected by the intrinsic curvature of the surface. Using the Tersoff [20] and T-B [21] potentials, Robertson et al. [35] showed that the elastic energy of a single-wall CNT scales as

$$\frac{1}{R^2}$$

where R is the radius of the tube. This is similar to the results deduced from the continuum elastic theory [36].

For axial strains, the Young's modulus of a SWNT is defined as

$$Y = \frac{1}{V} \frac{\partial^2 E}{\partial \varepsilon^2}$$

where E is the strain energy and V is the volume of the nanotube. Initial computational studies [33] using the same T-B potential reported the value of Young's modulus to be as high as 5.5 TPa. This was mainly due to a very small value of CNT wall thickness (~0.06 nm) used in this study [33]. It turns out that this was partly because of the attempts to use continuum theory to describe equivalence between a shell model and the atomistic descriptions of the elastic properties of CNTs. In many later works, this discrepancy [33] has been corrected.

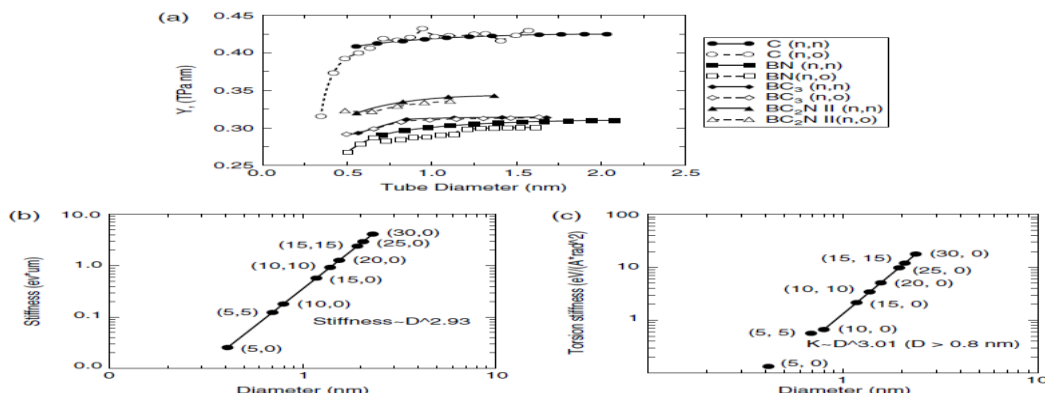


**FIGURE 2 Modulus of carbon nanotubes, (a) Young's modulus of C, BN, and other heteroatomic nanotubes. (From E. Hernandez et al. Phys. Rev. Lett. 80, 4502, 1998. With permission.) (b) Bending stiffness, and (c) torsion stiffness**

The bending stiffness of a single-wall CNT is defined as

$$\frac{1}{L} \frac{d^2 E}{d C^2}$$

where E is the total strain energy, L is the length, and C is the curvature of the bent nanotube, which is related with the bending angle  $\theta$  as

$$C = \frac{\theta}{L}$$

From the elastic theory of bending of beams, the strain energy of a bent nanotube can be expressed as

$$E = 0.5 Y h L \oint t^2 C^2 dl$$

where Y is the Young's modulus of the SWNT, and h is the thickness of the wall [42]. The integral is taken around the circumference of the nanotube, and t is distance of atoms from the central line (or the bent axis) of the tube. From this expression, the bending stiffness K is found to be equal to  $Yh(\pi r^3)$  and scales as cubic of the radius of the tube. Results from the molecular dynamics simulations, with Tersoff-Brenner potential, show that stiffness K scales as  $R^2.93$ , which is in good agreement with scaling predicted by the continuum elastic theory. The corresponding bending Young's modulus ( $Y_B$ ) of SWNT with varied diameters can be calculated from the above equation. For a small diameter SWNT,  $Y_B$  is found to be about 0.9 TPa, which is smaller than the

stretching Young's modulus calculated from the TB method or first principle theory. The computed smaller value is also similar to what Robertson et al.[34][35] showed in their study of the elastic energy of SWNTs, and the qualitative agreement is rather good. Poncharal et al. [43] have experimentally studied the bending Young's modulus of MWNTs (diameter >10 nm) using electrically induced force and found that the bending Young's modulus is in the range of GPa and decreases sharply with the increase in tube diameter. The large angle bending of SWNTs and MWNTs leads to elastic collapse of the structure that has been investigated in molecular dynamics simulations [44].

[36] The torsion stiffness of a CNT is defined as

$$K = \frac{1}{L} \frac{d^2 E}{d\theta^2}$$

where E is the total strain energy and  $\theta$  is the torsion angle. The shear strain is related with torsion angle as

$$\varepsilon = \frac{R\theta}{L}$$

where R is the radius of tube and L is its length. From continuum elastic theory, the total strain energy of a cylinder can be written as

$$E = \frac{1}{2} G * \iiint \varepsilon^2 dV$$

where G is shear modulus of the tube. The torsion stiffness thus is related with G as

$$K = \frac{1}{L} \frac{d^2 E}{d\theta^2} = G(2\pi h) \frac{R^3}{L^2}$$

where h is the thickness of the wall of the nanotube. The recently computed values of the torsional stiffness of several armchair and zigzag CNTs using T-B potential show the torsional stiffness to be about

$$0.1 \frac{eV}{A \text{rod}^2}$$

for (5,5) and (10,0) CNTs. This is in good agreement with the prediction of cubic dependence from the continuum elastic theory. The shear modulus of CNTs is found to be around 0.3 TPa and is not strongly dependent on diameters (for D > 0.8 nm). This value is smaller than that of about 0.45 TPa in Reference 37 calculated with an empirical force constant model. For small diameter tubes, such as a (5,5) nanotube, the shear modulus deviates from the continuum elastic theory description.

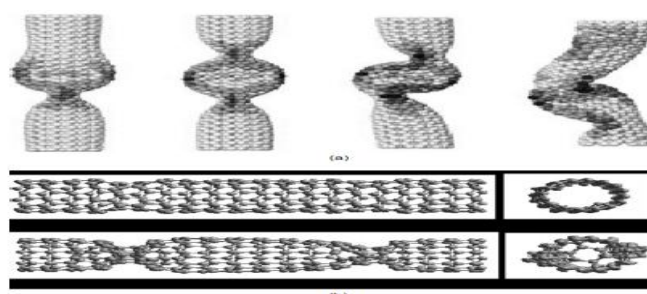


**FIGURE 3 (a)Collapse of CNTs under compressive strain with (a) sideways buckling or fin-like structures under elastic limit. (b)Local plastic collapse of the structure driven by graphitic to diamond-like bonding transition at the location of the collapse while the CNT remains essentially straight.**

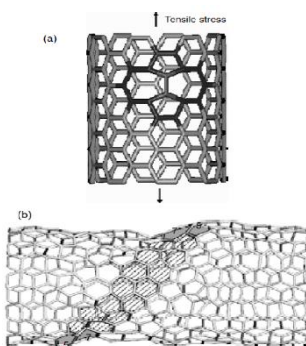


**FIGURE 4 (a) Configuration of a Stone-Wales defect that initiates the plastic collapse of a CNT under tensile strain [56], and (b) a series of SW defects form and slide apart from each other as CNT is continued to be stretched**

#### **4.2. Buckling, Collapse, and Plasticity of Carbon Nanotubes**

As the axial strain is increased gradually to more than a few percent, nanotubes have been observed to undergo two kinds of structural changes. First, under compressive strains, nanotubes exhibit structural instabilities resulting in the sideways buckling and collapse (flattening into fin like structures) of the structure, but the deformed tubular structure remains within elastic limit for more than 20% compressive strain [33]. Experiments have shown sideways buckling, collapse, and breaking feature in compressed and tensile stretched MWNTs in polymer composite materials [45,46]. The positions of these deformations can be well predicted with continuum mechanics based description of CNTs, and a reasonable comparison with MD simulations using T-B potential is obtained [33]. Recently, more extensive MD simulations at higher temperatures [47] and simulations with higher accuracy tight binding molecular dynamics methods [40] showed that the above results [33] were inherently limited by the shortcomings of continuum mechanics based approaches. Specifically, in the same experiment on compressed MWNT in a polymer composite [45], another mode of plastic deformation of compressed thin nanotubes was observed, where the CNTs remain essentially straight but the structure locally collapses at large compression. Srivastava et al. [40] used a non orthogonal tight binding molecular dynamics method, and found that within Euler buckling length limitation a straight CNT can locally collapse without undergoing either sideways buckling modes or through formation of fin like structures. The local plastic collapse is due to a graphitic ( $sp^2$ ) to diamond-like ( $sp^3$ ) bonding transition at the location of the collapse, which is driven by a compressive pressure as high as 150 GPa at the location of the collapse.

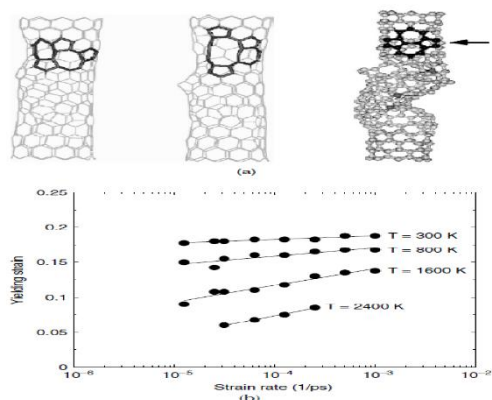


**FIGURE 5** The yielding strain of a CNT under tension is sensitive to temperature and the rate at which the strain is applied, (a) a tensile strained CNT at two different temperatures yield at different strains and with different type of structural defects, (b) yielding strain of a CNT as a function of strain rate varying over 3 orders of magnitude and temperature. [56].

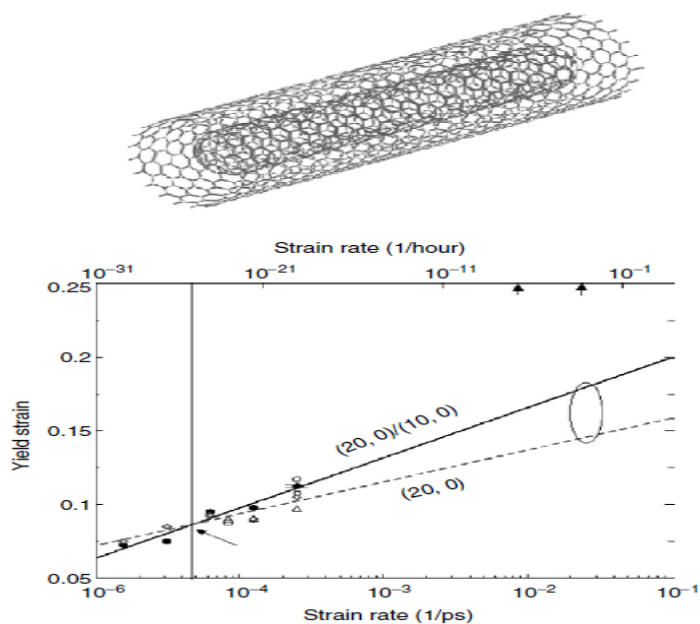


**FIGURE 6** The yielding strain of a multiwall CNT through a model of a double wall CNT where the contact is made only on the outermost wall (top), and the yielding strain of the double-wall CNT as a function of strain rate (bottom). The experimentally feasible strain rate and yielding strain is indicated with the elliptical area [57].

#### 4.3. Simulations of Vibrational and Thermal Properties

The small and large amplitude nanomechanics of CNTs described above focuses on the strength and stiffness characterization as well as mechanism and rate of the failure of the nanotubes under external load. Very small amplitude harmonic displacements of C atoms from their equilibrium position, on the other hand, keep the structural integrity but are mainly responsible for the vibrational and thermal properties of CNTs. In this section,

a brief summary on the simulations of vibrational or phonon spectra and thermal conductivity and heat pulse propagation in CNTs is provided. The simulated phonon and vibrational spectra of any newly discovered material are generally useful for characterization and were simulated first to identify and assign the peaks in resonance Raman experiments on CNTs [58]. The phonon spectrum is obtained by constructing and diagonalizing dynamical matrix from position dependent interatomic force constants. The eigen values of the dynamic matrix gives the frequency of vibrations, and the corresponding eigen vectors give nature of the corresponding modes of the vibration for atoms within a unit cell. The accuracy of the computed vibrational or phonon spectra at 0 K obviously depends on the accuracy of the interatomic forces used in constructing the dynamical matrix. Many studies on the zero temperature vibrational or phonon spectra of CNTs using the ab-initio density functional [38], tight-binding [58–61], and harmonic spring constants satisfying hooke's law [62] have appeared. Agreement between the experimental peaks and the zero temperature vibrational peaks is generally good because only the configurations at or very close to equilibrium structures are investigated. Thermal transport through CNTs, on the other hand, is sensitive to the choice of good atomic interaction potential, including the anharmonic part because the atomic displacements far from equilibrium positions are also sampled. The room temperature (300 K) phonon spectra or density of states and vibrational amplitudes have been computed recently [31]. The spectra were simulated through Fourier transform of temperature dependent velocity autocorrelation functions computed from MD trajectories using T-B potential for C–C interactions [20,21]. Good agreement with zero temperature phonon spectra, computed with higher accuracy ab initio DFT and TB methods, [38,58–61], was obtained. Additionally, the line width of the computed spectra provides temperature dependent life and correlation time of the phonon excitations involved. The spectra were used to assign the low-frequency Raman modes of CNT bundles as well [31].

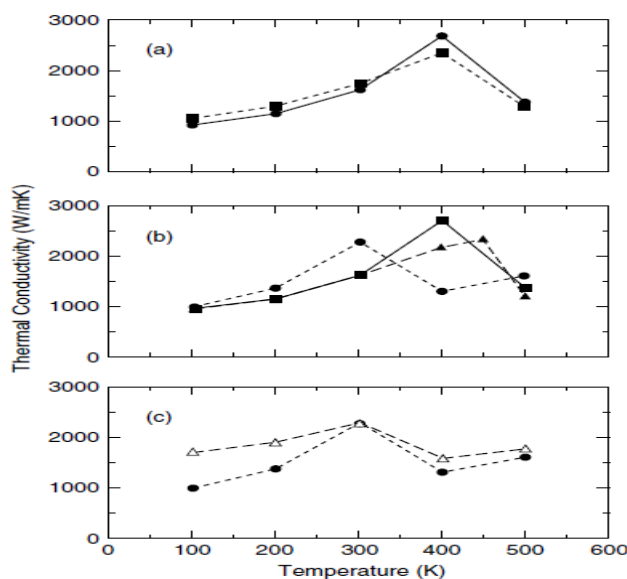


**FIGURE 7 The direct MD-simulated thermal conductivity of CNTs as a function of strain rate with (a) comparison between a (10,10) nanotube and graphene sheet; (b) a comparison between (5,5), (10,10), and (15,15) nanotubes; and (c) a comparison between a (5,5) and (10,0) nanotubes**

#### **4.4. Mesoscopic Scale Simulations of CNTs**

The simulations of individual CNTs and CNT reinforced polymer composites described so far are done with MD simulation methods where the advantage is that the structure and dynamics can be described very accurately at the atomistic level. Even electronic or quantum effects can be incorporated by using the interatomic force fields described by more accurate TB or ab initio DFT approaches. The limitations are that, on a regular basis, simulations with millions of atoms are not feasible when long range or large size structural, dynamic, and temporal effects are incorporated. Such effects may determine the characteristic behavior in composites involving bundles of CNTs, MWNTs, or dispersion-diffusion of many SWNTs. These issues are important from both the processing and the applications point of view. A bridge to macroscopic size systems is feasible through continuum mechanics based approaches, but such approaches generally neglect all atomic and molecular level interactions that could primarily determine the much promised novel application capabilities of these nanostructured materials. In the intermediate “mesoscopic” (~ a few hundred nanometers) length scale regime, therefore, CNTs and composites are generally “too large” to be simulated with quantum or atomistic approaches on a regular basis and are “too small” for the direct applicability or even accuracy of the methods based on continuum mechanics. It turns out that currently there are no mesoscopic structural and dynamic methods especially suited for CNTs or composites based on CNTs. There have been some attempts to find an equivalence between the large scale “structural mechanics” that is based on beams and struts and the atomistic scale “molecular mechanics” based on atoms and bonds. A preliminary hybrid approach, “molecular structural mechanics,” has been developed. So far it has been applied only for static structural simulations, and it is not clear how much computational efficacy is achieved when individual atoms and molecules are replaced by equivalent but individual struts and beams in the alternative description [70].

#### **V. CONCLUSION**

The examples discussed here provide a narrow window on a very broad field of applications and areas that are opening up and directly fueled by the efforts and advances in the computational nanotechnology based investigations of CNTs. Some of the covered areas and applications in this chapter include nanomechanics and thermal properties of CNTs and CNTs in polymer composite materials; chemical reactivity or functionalization of pristine or deformed nanotubes, gas physisorption, diffusion, and storage devices through CNTs, polymer translocation and diffusion in CNT nanochannels for sequencing or drug delivery applications; molecular electronic device components through nanotube heterojunctions and nanosensors for minuscule amounts of gas and biochemical detection applications, etc. In the future, it may be possible to conceptualize nanoscale synthetic machines and motors that could be powered and controlled through external laser, electric, or magnetic fields and operate in a chemical solution phase or inert gas environment. Such a concept of nanogears is shown in Figure 8. The design of the gears is based on the analogous chemical reactions that are known to occur in bulk phase chemistry. No fabrication pathway for making such nanoscale gears has been suggested to date. Computational modeling and simulation is useful to investigate the optimal structural, material, and operating conditions. The result of such investigations is that CNT-based nanogears, if made, could be more robust than

similar gears and other machines fabricated and operated in the macroworld. This is an example illustrating that the future of CNT based devices and systems can be shaped by the advances in computational nanotechnology.

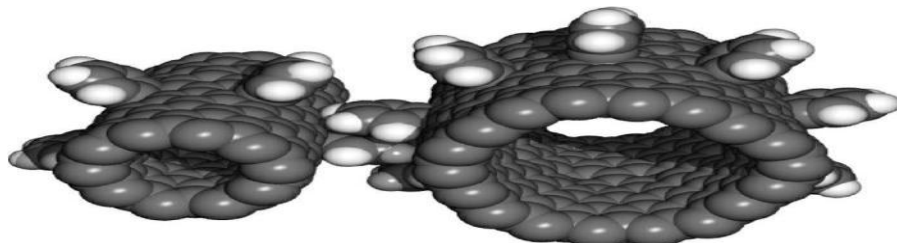


**FIGURE 8 CNT-based gears simulated at NASA Ames in the beginning of the program**

## REFERENCES

1. S. Iijima, Nature, 354, 56 (1991).
2. S. Iijima, Nature, 363, 603 (1993).
3. D.S. Bethune et al., Nature, 363, 605 (1993).
4. R. Saito, G. Dresselhaus, and M.S. Dresselhaus, Physical Properties of Carbon Nanotubes, Imperial College Press, London, (1998).
5. M.S. Dresselhaus, G. Dresselhaus, and Ph. Avouris, Eds., Carbon Nanotubes: Synthesis, Structure, Properties, and Applications, Springer-Verlag Berlin, Heidelberg, (2001).
6. M. Meyyappan and D. Srivastava, Carbon nanotubes, in Handbook on Nanoscience, Engineering and Technology, CRC Press, Boca Raton, FL, (2003). Chap. 18.
7. D. Srivastava, M. Menon, and K. Cho, Comput. Sci. Eng., 3, 42, (2001).
8. A. Nakano et al., Comput. Sci. Eng., 3, 56, (2001).
9. R.E. Rudd and J.Q. Broughton, Physica Status Solidi B, 217, 251, (2000).
10. M. Payne et al., Rev. Mod. Physics, 68, 1045, (1992).
11. P. Hohenberg and W. Kohn, Phys. Rev., 136, B864, (1964).
12. W. Kohn and L.J. Sham, Phys. Rev., 140, A1133, (1965).
13. J. Hafner, VAMP/VASP Guide, <http://cms.mpi.univie.ac.at/vasp> (current 5 June 2001), (1999).
14. R. Car and M. Parrinello, Phys. Rev. Lett., 55, 2471, (1985).
15. W. A. Harrison, Electronic Structure and Properties of Solids, W. H. Freeman, San Francisco, (1980).
16. M. Menon and K.R. Subbaswami, Phys. Rev. B, 55, 9231, (1997).
17. M. Menon, J. Chem. Phys., 114, 7731, (2001).
18. M.P. Allen and D.J. Tildsley, Computer Simulations of Liquids, Oxford Science Publications, Oxford, (1987).
19. B.J. Garrison and D. Srivastava, Ann. Rev. Physical Chem., 46, 373, (1995).
20. J. Tersoff, Phys. Rev. B, 39, 5566, (1989).
21. D.W. Brenner, O.A. Sherendova, and A. Areshkin, Quantum Based Analytic Interatomic Forces and Materials Simulations, Rev. in Comp. Chem., VCH Publishers, New York, 213, (1998).
22. D. Srivastava and S. Barnard, Molecular Dynamics Simulation of Large Scale Carbon Nanotubes on a Shared Memory Archi-tecture, Proc. IEEE Supercomputing 97 (SC '97 cd-rom), (1997).

23. S. Datta, Electronic Transport in Mesoscopic Systems, Cambridge University Press, Cambridge, (1995).
24. L. Chico et al., Phys. Rev. B, 54, 2600, (1996).
25. A. Andriotis, M. Menon, and G. E. Froudakis, Phys. Rev. Lett., 85, 3193, (2000).
26. A. Andriotis and M. Menon, J. Chem. Phys., 115, 2737, (2001).
27. A.N. Andriotis, M. Menon, and D. Srivastava, J. Chem. Phys., 117, 2836, (2002).
28. F. Muller-Plathe, J. Chem. Phys., 106, 6082, (1997).
29. M. Osman and D. Srivastava, Nanotechnology, 12, 21, (2001).
30. J.C. Tully et al., Phys. Rev. B, 31, 1184, (1985).
31. V.P. Sokhan, D. Nicholson, and N. Quirke, J. Chem. Phys., 113, 2007, (2000).
32. P.K. Schelling, S.R. Phillipott, and P. Kebinski, Phys. Rev. B, 65, 144306, (2002).
33. B.I. Yakobson, C.J. Brabec, and J. Bernholc, Phys. Rev. Lett., 76, 2511, (1996).
34. D. Srivastava, C. Wei, and K. Cho, Appl. Mech. Rev., 56, 215, (2003).
35. D.H. Robertson, D.W. Brenner, and J.W. Mintmire, Phys. Rev. B, 45, 12592, (1992).
36. G.G. Tibbetts, J. Cryst. Growth, 66, 632, (1994).
37. J.P. Lu, Phys. Rev. Lett., 79, 1297, (1997).
38. S. Portal, Phys. Rev. B, 59, 12678, (1999).
39. E. Hernandez et al., Phys. Rev. Lett., 80, 4502, (1998).
40. D. Srivastava, M. Menon, and K. Cho, Phys. Rev. Lett., 83, 2973, (1999).
41. V.M. Harik, Solid State Commun. 120, 331, (2001).
42. L.D. Landau and E.M. Lifschitz, Theory of Elasticity, 3rd ed., Pergamon Press, New York, (1986).
43. P. Poncharal et al., Science, 283, 1513, (1999).
44. S. Iijima et al., J. Chem. Phys., 104, 2089, (1996).
45. O. Lourie, D.M. Cox, and H.D. Wagner, Phys. Rev. Lett., 81, 1638, (1998).
46. O. Lourie and H.D. Wagner, Appl. Phys. Lett., 73, 3527, 1998.
47. C.Y. Wei, D. Srivastava, and K. Cho, Comput. Model. Eng. Sci., 3, 255, (2002).
48. D. Srivastava, M. Menon, and K. Cho, Phys. Rev. B, 63, 195413, (2001).
49. M.B. Nardelli, B.I. Yakobson, and J. Bernholc, Phys. Rev. Lett., 81, 4656, (1998).
50. P.H. Zhang, P.E. Lammert, and V.H. Crespi, Phys. Rev. Lett., 81, 5346, (1998).